



Universal screening platform using three-dimensional small molecule microarray based on surface plasmon resonance imaging

Journal:	<i>RSC Advances</i>
Manuscript ID	RA-ART-08-2015-015637.R2
Article Type:	Paper
Date Submitted by the Author:	25-Sep-2015
Complete List of Authors:	Singh, Vikramjeet; Shanghai Institute of Materia Medica, Chinese Academy of Science, Nand, Amita; National Center for Nanoscience and technology, Singh, Sarita; NIMS university Jaipur,
Subject area & keyword:	



Journal Name

ARTICLE

Universal screening platform using three-dimensional small molecule microarray based on surface plasmon resonance imaging

Received 00th January 20xx,
Accepted 00th January 20xx

DOI: 10.1039/x0xx00000x

www.rsc.org/

Vikramjeet Singh,^{a,b,c,*} Amita Nand^{b,c} and Sarita^d

Although much progress has been made in small molecule microarray in past decades, its potential has been limited by the lack of efficient methodology. Herein, we are reporting a potent methodology for the drug screening on a three-dimensional (3D) surface using carbene based photo-cross-linking reaction. The simultaneous display of a large number of small molecules on a single polymer chain in various orientations allows for the retention of their activity. The presented method was tested by using high-throughput surface plasmon resonance (SPRi) with the immunosuppressive drugs rapamycin and FK506. We showed that rapamycin and FK506 immobilized on the 3D surface, not the conventional 2D surface, bound to the FKBP with high affinity. Using FKBP-binding ligands and FKBP mutants with altered mutual binding affinities, we observed a strong correlation between the relative binding affinities determined by SPRi and those previously reported. In addition, other important parameters including, Blocking, washing, robustness and surface reproducibility were also validated. Some well known kinase inhibitors of p38 α , JNK and EK2 proteins were also used to extend the method applications. All together, these results suggested that the newly developed 3D small molecule microarray in conjunction with SPRi can be a powerful platform for high throughput drug screening.

Introduction

Small molecule microarrays (SMMs) has been extensively studied and updated after its initiation by Macbeath *et al* in 1999.¹ The field of SMMs is an exciting area of microarrays and enables the discovery of important and unexpected protein-ligand interaction that can result in therapeutic utility.² Small molecules can be further modified to become more efficacious and selective that can lead to therapeutic candidates. The biochemical evaluation of small molecules is an important first step in drug discovery pipeline.³ Small molecule microarrays can provide such compounds or leads, yet better protocols are still in need for the development and to be more widely used in high throughput screenings. Several challenges include the functional immobilization of the diverse and complex structural properties of the compounds to screen and the density of these compounds on the arrays which affects the sensitivity.

Several immobilization strategies including covalent, non-covalent and photo-cross linking capturing onto glass and the gold surface have been introduced.⁴⁻⁷ From all above, photo-cross-linking technique proved to be the most efficient technique due to non-selective and covalent immobilization of small molecules. Mainly 3-aryl-3-trifluoromethylidiazirines has been used as photo affinity labelling group to immobilized small molecules by generating a highly reactive species carbene upon exposure to the UV radiations.⁸ Previously, several researchers including Kanoh *et al.* reported non-selective (photo-cross-linking) method for immobilization of small molecules on 2D photo cross linked (PCL) surface (glass and gold).⁹⁻¹⁰ 2D surface was predominantly used for the preparation of SMMs provided

satisfactory results for common inhibitors against their specific antibodies. Although, 2D PCL surface can be easily prepared, they own low loading capacity that results in sensitivity issues. To overcome these limitations, Marsden *et al.* described a 3D hydrogel surface for selective immobilization which owns a high loading capacity that enhances the sensitivity and reduces non-specific adsorption of proteins.¹¹ Recently, we have made a major contribution in the improvement of loading capacity and sensitivity of SMMs by using cyclodextrin substrate in conjugation with surface plasmon resonance imaging (SPRi).¹² Conventional HTS detection method such as TR-FRET, Fluorescence polarization and ALPHAscreen face equivalent challenges due to a number of limitations such as fluorescence interference, protein labeling, small molecule solubility, and lengthy analysis times. Therefore, an alternative label free detection technology can be significantly advantageous. A great advantage of SPRi over classical SPR technique¹³ is high throughput, allowing the parallel evaluation of hundreds or thousands of compounds simultaneously.¹⁴ Moreover it provides a rapid identification of biomolecular interactions along with their kinetic parameters in real time.¹⁵ A variety of small molecules have been reported on SPRi for measuring protein-ligand interaction and protein-protein inhibition.¹⁶

In this article, a well established polymer brush via surface initiated polymerization (SIP) 3D surface from low initiator density in controlled manner was used as a platform (Fig. 1). SIP was successfully used by Ma *et al.* to detect biomolecular interaction with SPR and other biosensors techniques.¹⁷ A combination of SMMs and SPRi has been used to detect ligand-protein interaction and benchmark them against those reported in the literature. In our recent study for the comparison of non-specific adsorption and immobilization capacity, SIP surface produced better results when compared to the other 3D platforms for biosensor applications.¹⁸ To use the superiority of SIP platform, we have assembled the photo-cross-linking moiety over the SIP substrate. As expected, the obtained results were more than satisfactory in terms of sensitivity, specificity and reproducibility. The performance of the reported platform was tested by fluorescence and SPRi. In addition with some well know small molecule-protein interactions (FKBP and kinase binding ligands), 6 different mutants of FKBP12 protein, D37V, F48L, W59A, W59L, Y26F and Y26F82F were also included to prove versatility of the surface in SMMs format.¹⁹ In order to provide an ideal SMMs platform, surface were thoroughly evaluated for all

^a Center for Drug Delivery System, Shanghai Institute of Materia Medica, Chinese Academy of Sciences, Shanghai 201203, China.

^b National Center for Nanoscience and Technology, Beijing 100190, People's Republic of China.

^c University of Chinese Academy of Sciences, 100049, Beijing, People's Republic of China.

^d NIMS University Jaipur, 303121, Rajasthan, India

† Footnotes relating to the title and/or authors should appear here.

Electronic Supplementary Information (ESI) available: See DOI: 10.1039/x0xx00000x

necessary parameters including, UV irradiation time, washing and regeneration processes.

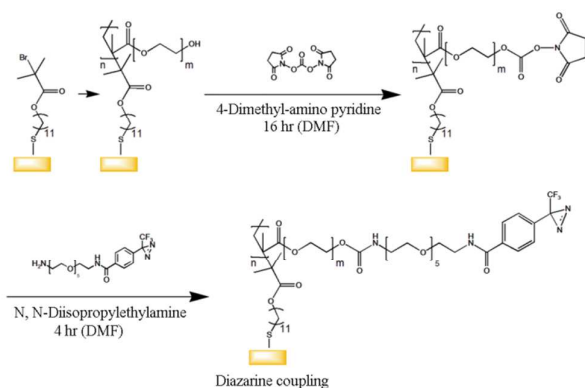


Fig. 1. A schematic representing the fabrication of 3D surface initiated polymerization based photo-cross-linking surface

Results and Discussion

XPS analysis and comparison of 2D PEG and 3D SIP PCL surfaces by Fluorescence

First of all, FTIR and XPS techniques were used for structure confirmation and the immobilization of photo-cross-linking moiety respectively. FTIR results (Fig. 2) confirmed the successful fabrication of PEG and SIP substrate onto gold surfaces. The obtained results from XPS indicated the presence of high amount of F and N elements on the surfaces which proved the presence of photo-cross-linking group (Table S-1). To check the high loading capacity of 3D SIP, a standard experiment was carried out to compare 3D SIP with 2D PCL surfaces using fluorescence detection technique. In order to compare the reactivity and capacity of both surfaces, rhodamine B, a well known fluorescence dye was used as a reference compound.²⁰ Slides were evaluated in terms of signal intensity and spot morphology. Scanned images of 2D and 3D PCL surfaces by fluorescence microscope were shown in Fig. 3a. The background corrected rhodamine B intensity from 2D and 3D PCL surfaces were plotted against each other at 3 different concentrations (Fig. 3b). The 3D PCL slides produced on average approximately 5 times higher intensity over 2D PCL slides. As a negative control, rhodamine B showed very little non-specific adsorption on both surfaces. In addition with high loading capacity, the 3D SIP slide also produced more consistent spot morphology in terms of both size and shape of the spots when compared to the 2D PCL slide. In support, images from SPRI instrument (before washing procedure) were presented in Fig. S-1 for the comparison of spot morphologies over both the surfaces. A regular spot morphology is particularly important in the selection of the spots during the experiments and data analysis which affects the data quality and surface reproducibility.

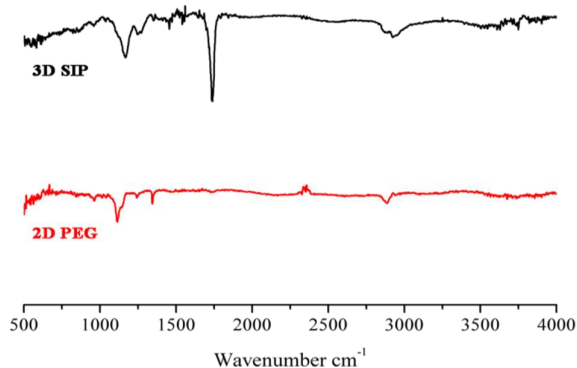


Fig. 2. FTIR spectra of 3D SIP and 2D PEG surfaces after acidification

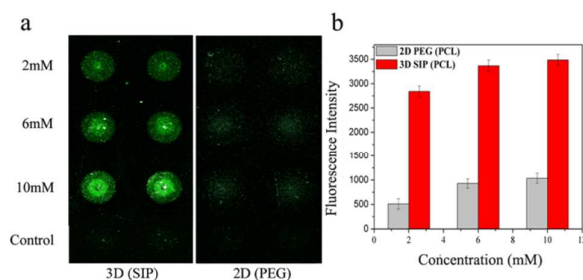


Fig. 3. Loading capacity comparison by fluorescence microscopy (a) Image showing signal intensities of rhodamine B at three different concentrations (2, 6 and 10mM) with control (without photo-cross-linker) and measured at 532 PMT gain. (b) Plot of three different concentrations from 2D (PEG) and 3D (SIP) PCL surfaces and showing approximately 5 times higher signal intensities in case of 3D than 2D surface.

Surface evaluation

To present an ideal methodology, it is very necessary to check the key parameters in each and every aspect. Washing of microarray and removal of bound proteins (regeneration) from the platform had major impact on data quality and microarray efficiency. Missing of any key point could be easily misleading and therefore, presented surface was evaluated very carefully in terms of UV irradiation time, washing and regeneration steps.

In previous reports, microarrays were irradiated under UV for 30 minutes which was very long and definitely not good for some sensitive small molecules structures. In order to validate, 5 chips were printed with rapamycin under identical conditions and irradiated for 0, 10, 20, 30 and 40 minutes. Interaction was measured by flowing FKBP12 (same concentration) and as expected, no signals were observed from 0 minutes and rest of slides showed not much difference (Fig. S-2) in signals intensities. Results suggested that, 10 minutes was enough to crosslink the small molecules onto SMMS platform.

Rapamycin and FK506 were chosen to validate the washing step. As shown in Fig. S-3, FKBP12 protein flowed on improperly washed spots (10 minutes in DMF) of rapamycin and FK506, continuous losing of precipitated and physically adsorbed molecules resulted into subsequent decrease in baseline level which finally affect the kinetics of rapamycin (11.7 nM) and FK506 (9.3 nM). Same test was carried out on properly washed spots (30 minutes (ultrasonic) in DMSO, DMF, ACN, ethanol, PBST and finally with distilled water) and found stable baseline and dramatic change in produced kinetics of rapamycin (1.19 nM) and FK506 (1.98 nM) showed good compatibility with original values.

Regeneration is also a key step in SPRI experiments to reuse the chip for next cycles and to obtain accurate kinetics. To check the regeneration, FKBP12 and D37V mutant proteins (possessing different binding affinities with rapamycin) were flowed against immobilized rapamycin molecules and regenerated with 10 mM solution of NaOH at different time spans. Due to weak binding affinity, D37V mutant could be easily regenerated at short span of regeneration (600sec) and no difference was recorded when compared to 1000 sec. In reverse, short regeneration cycle was unable to remove the wild type of FKBP12 protein due to strong binding affinity with rapamycin but successfully removed by long regeneration step of 1000 sec (Fig. S-4). Although, the long regeneration steps also affects the surface efficiency but very necessary to produce quality data. The obtained data suggested that the same regeneration solution and time span cannot apply on all interactions and need to adjust accordingly.

Comparison of surface sensitivity by SPRI

Several small molecules with weak and strong binding affinities with their relative target proteins were chosen to compare the 2 different surfaces. The chips with both surfaces (poly-ethylene-glycol and SIP) were fabricated with the photo-cross-linked group to capture different small molecules. Each

protein was subsequently flowed as analyte through the flow cell at single concentration of 100nM by setting 300sec association and 400sec dissociation phase separated by a single regeneration step. The response signals of biotin-streptavidin interaction (Fig. 4a) from the 3D PCL surface were significantly higher than 2D PCL. This effect was observed even more clearly for rapamycin and FK506 (Fig. 4b). No signal was observed without UV irradiation (data not shown), suggested that obtained signals were originated from covalently linked small molecules.

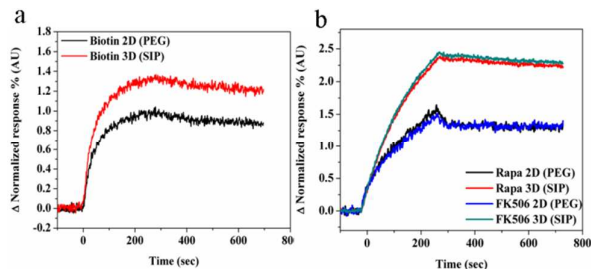


Fig. 4. Comparison of (a) biotin-streptavidin and (b) FKBP12 binding ligand interactions over 2D PEG and 3D SIP surfaces by SPRi

During the analysis of above described interactions, an average 0.5 to 0.7 times for biotin and 3-4 times for rapa and FK506 of signal enhancement were recorded from 3D SIP over 2D PEG photo-cross-linked surface. A large difference in signal enhancement of streptavidin and FKBP12 protein might be due to the difference in molecular weights of proteins and binding ligands.

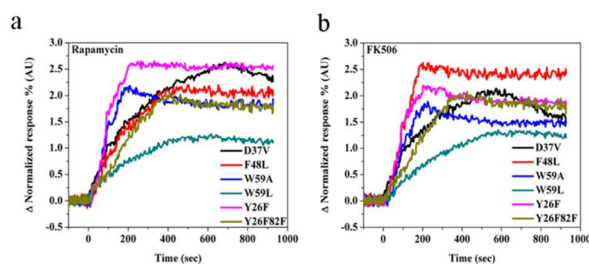


Fig. 5. Sensorgram showing interactions of six site directed FKBP12 with (a) rapamycin and (b) FK506

Furthermore, to prove the surface versatility, six site directed mutants (D37V, F48L, W59A, W59L, Y26F and, Y26F82F) of FKBP12 protein binds to Rapa and FK506 with wide range of affinities were expressed and selected for testing on the reported surface.²¹ Each selected mutant possessing specific and different binding affinity with rapamycin and FK506 compounds. As shown in Fig. 5a and Fig. 5b, the binding behaviour and response signals of all six mutants clearly showing the differentiation in according to their original behaviour. Using FKBP12 mutants with altered mutual binding affinities, we observed a strong correlation (Fig. 7a and Fig. 7b) between the relative binding affinities determined by SPRi and those previously reported by fluorescence titration assay (Table 1). Due to very low binding affinities of some of the mutants with FKBP12 binding ligands, data from 2D PCL slide was not considered for comparison. The above discussed data provided the clear information about the super performance of proposed SMM platform.

Proteins	KD (nM) Rapa Fluorescence titration	KD (nM) Rapa SPRi assay	KD (nM) FK506 Fluorescence titration ¹⁹	KD (nM) FK506 SPRi assay
W59A	28±16	12.3±4.32	50±31	64±6.09
W59L	2±2	2.45±3.01	46.0±5.3	30.1±4.75
Y26F	4.5±2.5	8.32±3.61	22.0±5.6	21.2±4.81
Y26F/Y82F	20.0±4.5	16.1±2.43	10.0±5.4	15.1±3.15
F48L	3.0±1.2	9.9±2.62	40±1.5	13.6±2.13
D37V	36.0±5.8	55.4±7.07	350±59	182.6±6.03

Table 1. Kinetics parameters of all six mutants against rapamycin and FK506 obtained from SPRi (3D SIP) in comparison with fluorescence titration assay.

Identification and comparison of kinase inhibitors interactions

After evaluating the above explained common interactions, we were interested to know whether this technique could also be applicable for measuring the interactions of proteins carrying deep binding pockets like cyclodextrin platform.¹² In this direction, some important and well studied kinase inhibitors were taken into account which represent interesting targets for many therapeutic areas. Kinase proteins have emerged as key component in most signal transduction cascades that researcher are constantly screening for better inhibitors.²² Until now, only a small number of kinases have been targeted by small molecule inhibitors and there is urgent need to develop strategies for efficient screening of new inhibitors.²³ The majority of these molecules binds to the highly conserved ATP pocket or other specified pockets which are deeper than the previous tested FKBP12 and streptavidin proteins.^{24, 25} Three well characterized protein kinases, p38α, ERK2 and JNK1 were chosen for this study. Four well known inhibitors of p38α (SB 202190, SB 239063, SB 203580 and EO 1428), two ERK2 inhibitors (TCS erk 11e and Kenpaullone) and two JNK1 inhibitors (BI 78D3 and SP 600125) were printed on the sensor chips in multiplex as described in methods.²⁶⁻³² All of three relative proteins were flowed in sequence through the flow cell at a single concentration (2μM) on the same slide. The binding signals for the p38α inhibitors from 2D PCL were significantly lower or negligible when compared to the 3D SIP surface (Figure S-5a and S-5b). The same behaviour was also observed with the other kinase-inhibitors combinations (Fig S-5c and S-5d) from 2D than 3D PCL surface. As shown in Figure S-5, all kinase interactions were successfully identified on 3D PCL surface and each inhibitor exclusively interacted with their relative target protein. The dramatic difference in signal intensities between 2D and 3D PCL surface can be well explained. Very low or negligible signal response was observed from 2D PCL surface for every kinase interaction could be due to the low immobilization capacity and deep binding pockets of target proteins. Due to which, molecules linked to the PEG chain are not capable to get inside into deep binding pockets of kinases. Above all, 3D PCL surface inherited the high immobilization capacity from 2D PCL surface but with one great advantage of screening of proteins with deep binding pocket in high throughput manner. A whole screening chart comparing mutants and other interactions was presented in Figure 6, Response shown here is at a single concentration of each protein on both the surfaces.

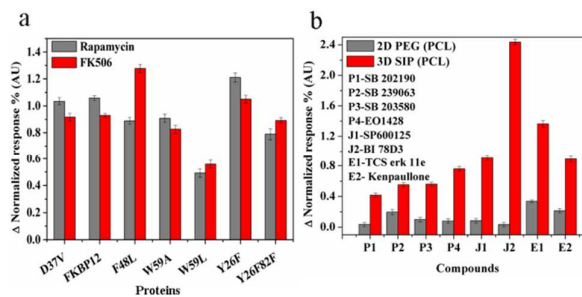


Fig. 6. SPRi response comparison for (a) FKBP12 mutants and (b) kinase inhibitors against their relative targets.

Bio-kinetic analysis of small molecules-protein interactions

For every screening, it is important to determine the weak as well as the strong binding interactions. We checked the 3D PCL surface performance in terms of uniformity and kinetics deviations from different experiments with multiple concentrations of each target protein. Surface reproducibility was also checked by measuring the kinetics of rapamycin and FK506 against FKBP12 protein. Rapamycin and FK506 were spotted (20 spots of each) over whole print area and measured affinities (Table S-2) suggested the high reproducible nature of the surface. It was observed that the dissociation rates from the 3D PCL slides are much slower especially in the case of rapa-FKBP12 and FK506-FKBP12 with KD values much closer to the literature (Table 2). The dissociation constants for FK506 and rapamycin obtained from different methods (literatures) were compared with those obtained from SPRi assay, a strong correlation can be observed between affinities

obtained from the 3D surface, but not the 2D surface (Table 2). The produced data together suggested that, potential of the reported surface is not only limited to the interaction identification but also can provide accurate kinetics parameters.

Compounds	Target protein	KD (nM) Literature ³³	KD (nM) 2D (SPRI)	KD (nM) 3D (SPRI)
Rapamycin	FKBP12	0.2	17.5±4.2	1.61±1.13
FK506	FKBP12	0.4	26.6±4.22	1.73±1.24

Table 2. Kinetic parameters of FKBP binding ligands obtained from SPRI (2D and 3D PCL) in comparison with chemical denaturation assay.

For kinase interactions, we choose not to measure kinetics for 2D PCL surface due to very low or negligible signal responses. The kinetic data for all kinase inhibitors obtained by using SPRI was also compared to the K_i /KD/IC₅₀ values reported from the literature in Table 3. The difference between SPRI and literature values might be due to the nature of binding constants compared, as affinity values of all these inhibitors were measured by using different *in vitro* and *in vivo* assays. In some cases, this difference is significant and might be due to high density of immobilized molecules and dense structure of the SIP surface.

Compounds	Target protein	KD (nM) SPRI	K_i /KD/IC ₅₀ (nM) Literature
SB 239063	P38 α	44.8±5.14	44
SB 202190	P38 α	56±4.72	50
SB 203580	P38 α	173±6.03	50
EO 1428	P38 α	93±4.80	4
SP600125	JNK1	7.61±5.61	40-90
BI 78D3	JNK1	11.6±2.24	280
TCS erk 11e	ERK2	25.5±2.11	<2
Kenpaullone	ERK2	360±8.80	900

Table 3. Kinetics parameters of kinase inhibitors from SPRI assay in comparison with IC₅₀ values from literature

Detailed kinetic parameters (avg. of 3 conc.) of FKBP12 and kinase interactions were presented in Table S-3, S-4, S-5, S-6 and S-7. Taking all this data into consideration, we could infer that the 3D SIP PCL surface in conjugation with SPRI seems very suitable to screen wide range of interactions in high throughput manner.

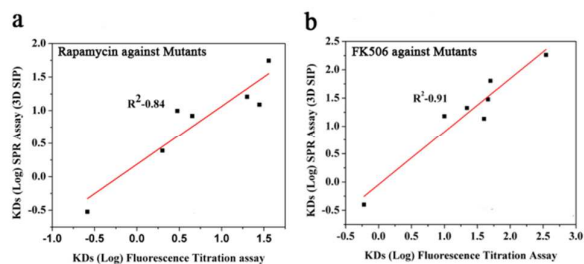


Fig. 7. Graph showing kinetics parameters correlation of FKBP12 mutants against (a) rapamycin and (b) FK506 obtained from 3D SIP surfaces with fluorescence titration assay

Conclusions

A high-throughput method for rapid detection of small molecule-protein interaction is a missing link for the exploitation of the drug screening against various protein targets. We present a 3D photo-cross-linking methodology for high-throughput screening of small molecule inhibitors to fill this technology gap. Several well known small molecule-protein interactions including kinase inhibitors were successfully examined. The reported platform was compared with 2D surface in every aspect and significant improvement in immobilization, sensitivity and kinetics parameters was recorded. The platform was carefully validated in terms of reproducibility,

sensitivity, specificity, regeneration and washing parameters. The ability to differentiate the specificity between same proteins with altered binding pockets made it more special and superior over all previously reported SMMs. Presented SMMs technology can be used for screening of thousands of small molecules against any protein targets, including cancer-driving mutants identified from cancer genome sequencing. This new methodology will provide an ideal screening platform that is capable of screening small molecule libraries against targets of interest. On the base of above discussed data we strongly believe that presented methodology will start a new revolution in small molecule microarray field.

Acknowledgements

We specially thank Prof. Jingsong Zhu for providing all instrumental facilities. We also would like to thank Prof. Yonghua Wang for providing lab to express and purify FKBP mutants and Prof. Jia-Wei Wu for providing high quality kinase proteins for validation of surface.

Experimental

Preparation of 3D polymer brush (SIP) surface

The SIP surface was prepared according to our previous published work.¹⁸ In brief, a mixed SAM solution was prepared by initiators ω -mercaptoundecyl bromoisobutyrate (BrC(CH₃)₂COO(CH₂)₁₁SH) and EG3-thiol in 1:99 ratio. The chips were immersed in this mixture (1mM total concentration) for 16 hours at room temperature, and then thoroughly washed by ethanol and Milli-Q water and dried in a nitrogen stream. Polymerization solution was prepared by 64mg Bipy, 10ml 0.04M CuCl₂, 2.6g HEMA, 7.2g OEGMA, 20ml Milli-Q water and 20ml methanol. After 30min deoxygenation, 10ml of AsCA (0.04M) were added to the solution and the chips were immersed in this solution for 16 hours at room temperature under an atmosphere of nitrogen. After being thoroughly washed with methanol and Milli-Q water, the chip were incubated in a DMF solution containing 0.1M DSC and 0.1M DMAP for 16 hour for acidification.

All kinase inhibitors were purchased from TOCRIS Bioscience. FKBP12 plasmid was a kind gift from Prof. Jun O. Liu from John Hopkins university.

SMMs preparation

The photo-cross-linker moiety (3-Trifluoromethyl diazarine) was synthesized according to previous reported protocol by Kanoh et al.⁹ PEG and SIP assembled slides were activated by freshly prepared aqueous mixture (1:1) of EDC/NHS solution for 20 minutes. Slides were then incubated with 100mM base added (500mM DIPEA) solution (DMF) of photo-cross-linker (20 μ l) and covered with cover slips and placed in the dark for 4 hours at room temperature.¹² Slides were then extensively washed with DMF for 30 minutes and blocked with 1M solution of ethanolamine in DMF. After washed with DMF and ethanol (10 minutes) and dried with N₂, slides were ready for printing. Stock solutions (10mM) in 100% DMSO were spotted in multiplex using a Genetix QArray 2 spotter (produced 300 μ m features) and left for complete evaporation of DMSO (under vacuum) at room temperature for 2 hrs. After printing, the slides were exposed to UV irradiation 2.4 J/cm² (365 nm) in a UV chamber (Amersham life science). The slides were subsequently washed with DMSO, DMF, ACN, ethanol, phosphate buffered saline (PBST) and finally with distilled water for 30 minutes (ultrasonically) respectively, to remove non-covalently bound compounds. Dried slides were assembled with flow cell and then mounted on SPRI instrument for measurement.

FTIR, X-ray photoelectron spectroscopy (XPS) and fluorescence method

Surfaces for XPS and fluorescence were fabricated according to above described fabrication procedure. Fourier transform infrared (FTIR) spectrophotometer (GX-Perkin Elmer, USA) was used at reflection mode at a resolution of 4 cm⁻¹ over the 4000–400 cm⁻¹ spectral region to reveal the chemical bond and functional groups such as carbonyl (C=O) and hydroxyl (OH) groups belonging to COOH-terminated alkanethiol SAMs. Element

analysis by XPS (ESCALAB 250Xi spectrometer, Thermo Fisher Scientific Co.) with the monochromatic Al K α X-rays source (1486.6 eV) was carried out to confirm and check the immobilization of photo-cross-linker moiety on surface. The spectrum was acquired at a takeoff angle of 0° with a 0.78mm² spot size at a pressure of less than 3×10⁻⁹ mbar. Further to compare the spot morphology and immobilization capacity by fluorescence method, different concentrations of rhodamine B (2mM, 6mM and 10mM) were spotted on area fabricated with and without linker as negative control on both 2D and 3D PCL surfaces under the same conditions in DMSO. Printed slides were washed subsequently with DMSO and ethanol in ultrasonic for 30 minutes each to remove physically adsorbed compounds and scanned for fluorescence (GenePix 4000B microarray scanner) at 532 PMT gain.

SPRI Method

All the experiments were carried out using the PlexArray® HT system (Plexera, LLC) which is based on surface plasmon resonance imaging.¹⁸ All samples were injected at the rate of 3μL/s and 25°C. Oval regions of interests (ROIs) were set as 12 pixels × 9 pixels area in imaging area. ROIs of biotin were used as controls for measurement of specific signals. Purified recombinant proteins diluted in PBST containing tween 20 (0.05%), pH 7.4 were used as analytes with an association and dissociation flow rate of 3μL/s at different concentrations by serial dilution. A solution of NaOH (10mM) was used to regenerate the surface and remove bound proteins from the small molecules enabling the sensor chip to be reused for additional analyte injections.

Binding experiments and data analysis

All small molecules were stored as stock solution in 100% dimethyl sulphoxide (DMSO) at -20°C. Protein samples were stored in PBST at -80°C. PBST was used as both analyte and running buffer. A typical sample injection cycle consists of 300 seconds association phase with the analyte solution and 400 seconds dissociation phase with running buffer at 3μL/s flow rate. Three different concentrations of FKBP12 (50, 100 and 200nM) and each kinase (500, 1000 and 2000nM) were used to flow onto the microarray to ensure accurate kinetics. All the experiments were repeated at least three times to ensure the data repeatability. Data was analyzed according to our previous work.¹⁸

References

- G. MacBeath, A. N. Koehler and S. L. Schreiber, *J. Am. Chem. Soc.*, 1999, 121, 7967–7968.
- A. J. Vegas, J. H. Fuller and A. N. Koehler, *Chem. Soc. Rev.*, 2008, 37, 1385–1394.
- D. Barnes-Seeman, S. B. Park, A. N. Koehler and S. L. Schreiber, *Angew. Chem., Int. Ed.*, 2003, 42, 2376–2379.
- F. G. Kuruvilla, A. F. Shamji, S. M. Sternson, P. J. Hergenrother and Schreiber, *Nature*, 2002, 416, 653–657.
- G. A. Korb, G. Lalic and M. D. Shair, *J. Am. Chem. Soc.*, 2001, 123, 361–362.
- K. S. Lam, R. Liu, S. Miyamoto, A. L. Lehman and J. M. Tuscano, *Acc. Chem. Res.*, 2003, 36, 370–377.
- J. E. Bradner, O. M. McPherson, R. Mazitschek, D. Barnes-Seeman, J. P. Shen, J. Dhaliwal, K. E. Stevenson, J. L. Duffner, S. B. Park, D. S. Neuberg, P. Nghiem, S. L. Schreiber and A. N. Koehler, *Chem. Biol.*, 2006, 13, 493–504.
- M. Platz, A. S. Admasu, S. Kwiatkowski, P. J. Crocker, N. Imai and D. S. Watt, *Bioconjugate Chem.*, 1991, 2, 337–341.
- N. Kanoh, K. Honda, S. Simizu, M. Muroi and H. Osada, *Angew. Chem., Int. Ed.*, 2005, 44, 3559–3562.
- N. Kanoh, M. Kyo, K. Inamori, A. Ando, A. Asami, A. Nakao and H. Osada, *Anal. Chem.*, 2006, 78, 2226–2230.
- D. M. Marsden, R. L. Nicholson, M. Ladlow and D. R. Spring, *Chem. Commun.*, 2009, 14, 7107–7109.
- V. Singh, A. Nand, Z. Cheng, M. Yang and J. Zhu, *RSC Adv.* <http://dx.doi.org/10.1039/C4RA07306A>.
- F. Pillet, C. Thibault, S. Bellon, E. Maillart, E. Trévisiol, C. Vieu, J. M. Francois and V. Anton-Leberre, *Sens. Actuators, B*, 2010, 147, 87–92.
- M. J. McDonnell, *Curr. Opin. Chem. Biol.*, 2001, 5, 572–577.
- O. S. Jung, H. S. Ro, H. S. Kho, Y. B. Shin, M. G. Kim and B. Chung, *Proteomics*, 2005, 5, 4427–4431.
- Y. Li, H. J. Lee and R. M. Corn, *Anal. Chem.*, 2007, 79, 1082–1088.
- H. Ma, J. He, X. Liu, J. Gan, G. Jin and J. Zhou, *ACS Appl Mater Interfaces*. 2010, 2, 3223–3230.
- V. Singh, A. Nand, Sarita, J. Zhang and J. Zhu, *Arab. J. Chem.* doi:10.1016/j.arabjc.2015.06.037
- M. T. DeCenzo, S.T. Park, B.P. Jarrett, R.A. Aldape, O. Futer, M.A. Murcko and D.J. Livingston, *Protein Eng.* 1996, 9, 173–180.
- P. Bartasun, H. Cieřliński, A. Bujacz, A. Wierzbicka-Woć and J. Kur, *PLoS One*, 2013, 8, e55697.
- F. Sun, P. Li, Y. Ding, L. Wang, M. Bartlam, C. Shu, B. Shen, H. Jiang, S. Li and Z. Rao, *Biophys. J.*, 2003, 85, 3194–3201.
- J. Zhang, P. L. Yang and N. S. Gray, *Nat. Rev. Cancer*, 2009, 9, 28–39.
- L. N. Johnson, E. D. Lowe, M. E. Noble and D. J. Owen, *FEBS Lett.*, 1998, 430, 1–11.
- P. Traxler and P. Furet, *Pharmacol. Ther.*, 1999, 82, 195–206.
- S. Nemoto, J. Xiang, S. Huang and A. J. Lin, *Biol. Chem.*, 1998, 273, 16415–16420.
- D. C. Underwood, R. R. Osborn, C. J. Kotzer, J. L. Adams, J. C. Lee, E. F. Webb, D. C. Carpenter, S. Bochnowicz, H. C. Thomas, D. W. Hay, D. E. Griswold and J. Pharmacol, *Exp. Ther.*, 2000, 293, 281–288.
- K. Sato, M. Hamanoue and K. J. Takamatsu, *Neurosci. Res.*, 2008, 86, 2179–2189.
- E. R. Ottosen, M. D. Sørensen, F. Bjørkling, T. Skak-Nielsen, M. S. Fjording, H. Aaes and L. J. Binderup, *Med. Chem.*, 2003, 46, 5651–5662.
- B. L. Bennett, D. T. Sasaki, B. W. Murray, E. C. O'Leary, S. T. Sakata, W. Xu, J. C. Leisten, A. Motiwala, S. Pierce, Y. Satoh, S. S. Bhagwat, A. M. Manning and D. W. Anderson, *Proc. Natl. Acad. Sci.*, 2001, 98, 13681–13686.
- J. L. Stebbins, S. K. De, T. Machleidt, B. Becattini, J. Vazquez, C. Kuntzen, L. H. Chen, J. F. Cellitti, M. Riel-Mehan, A. Emdadi, G. Solinas, M. Karin and M. Pellecchia, *Proc. Natl. Acad. Sci.*, 2008, 105, 16809–16813.
- A. M. Aronov, Q. Tang, G. Martinez-Botella, G. W. Bemis, J. Cao, G. Chen, N. P. Ewing, P. J. Ford, U. A. Germann, J. Green, M. R. Hale, M. Jacobs, J. W. Janetka, F. Maltais, W. Markland, M. N. Namchuk, S. Nanthakumar, S. Poondru, J. Straub, E. Haar and X. J. Xie, *Med. Chem.*, 2009, 52, 6362–6368.
- D. W. Zaharevitz, R. Gussio, M. Leost, A. M. Senderowicz, T. Lahusen, C. Kunick, L. Meijer and E. A. Sausville, *Cancer Res.*, 1999, 59, 2566–2569.
- W. S. Lane, A. Galat, M. W. Harding and S. L. Schreiber, *J. Protein Chem.*, 1991, 10, 151–160.